The North African Journal of Scientific Publishing (NAJSP)
مجلة شمال إفريقيا للنشر العلمي (NAJSP)
E-ISSN: 2959-4820
Volume 3, Issue 3, 2025
Page No: 265-279
Website: https://najsp.com/index.php/home/index
SJIFactor 2024: 5.49 معامل التأثير العربي (AIF) 2024: 0.71 ISI 2024: 0.696

Petrochemical Significance of Biotite Schist Xenolith from Jabal Fezzan, Southern Libya

Ali S. Ben Sera *
Department of Geology, Faculty of Science, University of Zintan, Zintan, Libya

الأهمية البتروكيميائية لصخور الزينوليت (بيوتايت شست) في جبل فزان، جنوب ليبيا

علي سالم علي بن صيرة *
قسم الجيولوجيا، الكلية العلوم، الجامعة الزنتان، الزنتان، ليبيا

*Corresponding author: a.bennasirh@uoz.edu.ly

Received: July 16, 2025	Accepted: August 22, 2025	Published: August 26, 2025

Abstract:
The Jabal Fezzan's xenolith has been intruded during Pan-African metamorphism, characterized by (high pressure and medium temperature), this process results in the formation of the biotite, muscovite, and kyanite metamorphic zones. There is a slight increase in the degree of metamorphism as it reaches the biotite zone. It consists of foliated, medium- to coarse-grained schists, mostly biotite, muscovite, and kyanite, additionally plagioclase and quartz, as well as zircon, rutile, and Fe oxides. The microscopical evidence indicates that iron-rich biotite in pelitic schists undergoes a series of chemical reactions that cause it to be formed and transformed into other minerals. P-T diagrams suggest that rocks in the study area might have been formed during collisions and decompressions of thickened continental crust. They are derived from sedimentary rocks such as greywacke, which contain high levels of Si_4^+ and Al_3^+. As P-T conditions pass through, the biotite isograd and biotite forms. This study highlighted the oldest metamorphic rocks in southern Libya, enhancing the understanding of the mantle source protolith metasomatism, and reducing the information gap between petrochemical significance and the evolutionary stage of Pan-African metamorphism in southern Libya through study xenolith outcrops in more detail.

Keywords: Isograd, Kyanite Metamorphic Zones, Pelitic Schist, Protolith Metasomatism.

الملخص
تشكلت الصخور الدخيلة في جبل فزان خلال عملية التحول الصخري للدرع الأفريقي، والتي تتميز بضغط عالٍ ودرجة حرارة متوسطة، مما أدى إلى تكوين مناطق تحول صخري من البايوتايت والموسكوفيت والكيانيت. هناك زيادة طفيفة في درجة التحول الصخري عند الوصول إلى منطقة البيوتايت. تتكون هذه الصخور من صخور شستية، متوسطة إلى خشنة الحبيبات، معظمها من البيوتايت والموسكوفيت والكيانيت، بالإضافة إلى البلاجيوكلاز والكوارتز، وكذلك الزركون والروتيل وأكاسيد الحديد. تشير الأدلة المجهرية إلى أن البيوتايت الغني بالحديد في الصخور الرسوبية و خضع لسلسلة من التفاعلات الكيميائية التي ادت إلى تكوينه وتحويله إلى معادن أخرى.كما تشير مخططات الضغط ودرجة الحرارة إلى أن الصخور في منطقة الدراسة ربما تكونت أثناء اصطدامات وانخفاضات ضغط القشرة القارية السميكة. وهي مشتقة من الصخور الرسوبية مثل الجرايوك، التي تحتوي على مستويات عالية من Si_4^+ و Al_3^+. تحت ظروف معينة من ضغط ودرجة حرارة، حيث تشكل البيوتايت الإيزوغرادي والبيوتايت. كما سلطت هذه الدراسة الضوء على أقدم الصخور المتحولة في جنوب ليبيا، مما عزز فهم التغير الصخري البروتوليتي لمصدر الوشاح، وتقليل من فجوة المعلومات بين الأهمية البتروكيماوية ومرحلة تطور التحول الصخري للدرع الأفريقي في جنوب ليبيا من خلال دراسة الصخور الدخيلة بمزيد من التفصيل.

الكلمات المفتاحية: إيسوغراد، مناطق متحولة الكيانيت، صخر شستي بيليتي، متحولة بروتوليثية.

Introduction

Libya's metamorphic history is inadequately documented. Some of the foreigners and Libyan geologists (e.g., Kilian 1925; Karpoff 1946; Leubre 1952; Wackrenier 1958; Menchikoff 1962; Freulon 1964; Greigert and Pougnet 1967; Hoen 1968; Klitzsch 1970; Klitzsch and Ziegert 2000; Schürmann 1974; Jurak 1978; Klerkx 1980; El Makhrouf 1988 ; El Makhrouf and Feiss (2012) ; Mamgain 1980; Oun et al., (1998) Peregi et al., 2003; Busrewil et al., 2006 and Oun and Busrewil (2012) have presented brief overviews of metamorphic events in southern Libya. Kilian (1925) described the metamorphic rocks in Libya as first time as Upper Proterozoic metamorphites. Later, Desio (1942,1943), who separated high-grade metamorphic rocks and accompanying intrusives as Archean.

According to Leubre (1952), he mentioned that there is only one metamorphic series of Middle-to-Upper Proterozoic age in the Sahara region. Wackrenier (1958) described them as consisting of quartzite, slate and salic lava. A current generally accepted opinion is that, according to age and composition, there are two different complexes of metamorphic formations in South Libya.The older complex, composed of rocks of high crystallinity, in the Jabal Eghi and Tibesti region, is made of high-grade metamorphites. The younger, low-grade metamorphic complex is exposed in Mourizidie area.Proteozoic metamorphites were dated as Middle-to Late Proterozoic (1.22-1.56 Ga) by Oun et al., (1998).

An excellent example is the Wadi Badran, which is composed of Proterozoic metamorphic rocks, which are the surface exposures of the Late Precambrian Pan-African orogeny intruded by syn- and late orogenic two-mica granite (Ben Sera 2024). It is important to highlight this study as an accurate reinterpretation of all previous geological studies related to Proterozoic metamorphic events in southern Libya as well as inside Jabal Fezzan. Wadi Badran from Jabal Fezzan (Figure 1), belonging to the greenschist facies (Peregi et al., 2003; Oun et al., 1998; Oun and Busrewil 2012; Ben Sera 2024) during the Pan-African orogeny, being older than the intruding syn- and post-tectonic granite of ca. 565-520 Ma and during the latest Neoproterozoic (Oun and Busrewil 2012).

Regional metamorphism is defined by a sequence of metamorphic zones including biotite and kyanite. It is composed of biotite-schist xenolith, with a dimension that varies from a few millimeters to several centimeters. In the metamorphic rocks of the Jabal Fezzan, a regional retrograde metamorphism is evident during granite emplacement, indicating a complex metamorphic history. The study area consists of two-mica granite (554–520 Ma (K/Ar); Jurk, 1978, (640–549 Ma (Rb/Sr); Schürmann, 1974), and the intermediate composition rocks (phonolite, nepheline-rich phonolite, poor nepheline trachyte (24 Ma (K/Ar); Jurk, 1978, and metapeltic rocks). The focus of this study is on semi-to-metapeltic rocks that contain biotite schist.

These rocks are a component of low- to medium-grade regional metamorphic rocks and have been observed to record conditions of 300–450 °C and 1–2.0 kbar in a diverse range of P-T conditions; it is possible for them to grow through a variety of reactions. In this study, Fe-rich biotite is described from pelitic schists located in Jabal Fezzan. A mineral assemblage combined with textural and phase equilibrium, along with evidence of metamorphism during early crystallization, results in polymetamorphism in this metamorphic unit. P-T pseudosection modeling is used to further understand biotite schist metamorphism.

Geological setting

The Precambrian rocks located in the south-central region of Libya, are exposed across an area not exceeding 3,000 square kilometers. Main exposures are located in the central and southern parts of Libya, particularly in the Jabal Eghei and Tibesti areas, a near the Sudan-Egyptian border in the Jabal Awenat-Jabal Arkenu areas, as well as Jabal Fezzan (JF). These rocks are comprised of gray muscovite and biotite granites that are intersected by dikes and veins of rhyolite and aplite porphyry. Crystalline and metamorphic rock account for less than 1 percent of Libya's total land area. They include para- and orthogneiss, quartzite, schist, phyllite, diorite, granite and granodiorite. It is postulated that these rocks are constituents of the basement complex and are regarded as analogous to the Pharusian. All of these rocks are associated with significantly folded quartzites, schists, and phyllites exhibiting a variety of colors. The Jabal Fezzan is located in southern part of Libya, ranges stretching in a north-south direction, attains, in its central part, more than 1km above sea level (Figure 1).

From the structural point of view, the origin of these Jabel is predisposed by the transversal vaulting of the large (Gargaf uplift) regional structure (Figure 2a). It's constituted of outcrops of the monotonous sandstone of the Hasawanah Formation (Figure 2b). The country rocks have a jointed cleavage and laminate structure; the cleavage strikes ENE-WSW (Figure 2a). The JF was affected by major uplift structures, mainly the Gargaf uplift trend ENE-WSW (Ben Sera 2024) and the Tibesti-Tripoli uplift of the north-south trend Jurk, 1978; ; Klitzsch, and Ziegert (2000). Joints and faults largely dominated the Cambrian structural stage in southern Libya, mainly displaying the Gargaf structural trend E–W (Figure 2a). Morphologically, the Jabal Fezzan is characterized by sharp crests or cones and deeply canyon-

like incised wadis. In the marginal parts of the Jabal Fezzan range, comparatively extensive fan-shaped Quaternary deposits occur. In the east and west, the Jabal Fezzan passes rapidly into the Gargaf plain, which also consists of extensive outcrops of the Hasawanah Formation.

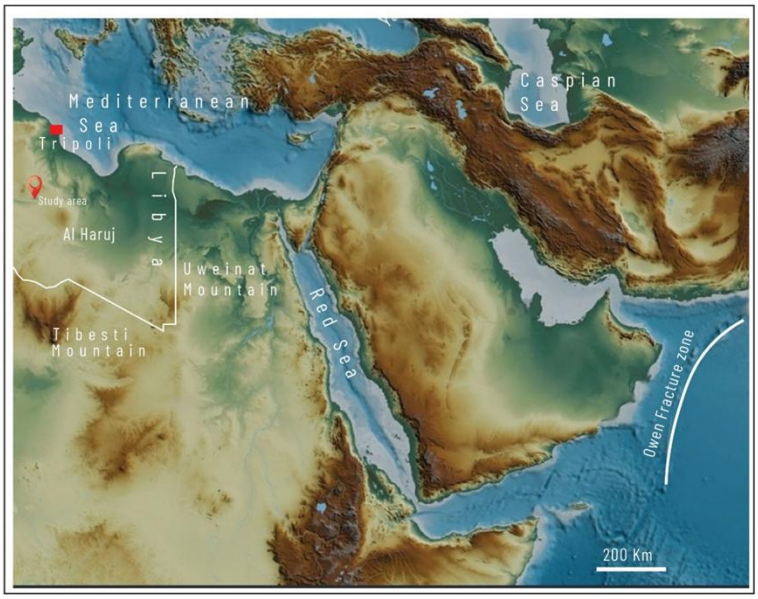

Figure1: 3d render of relief map of the study area modified after (source: shutterstock.com).

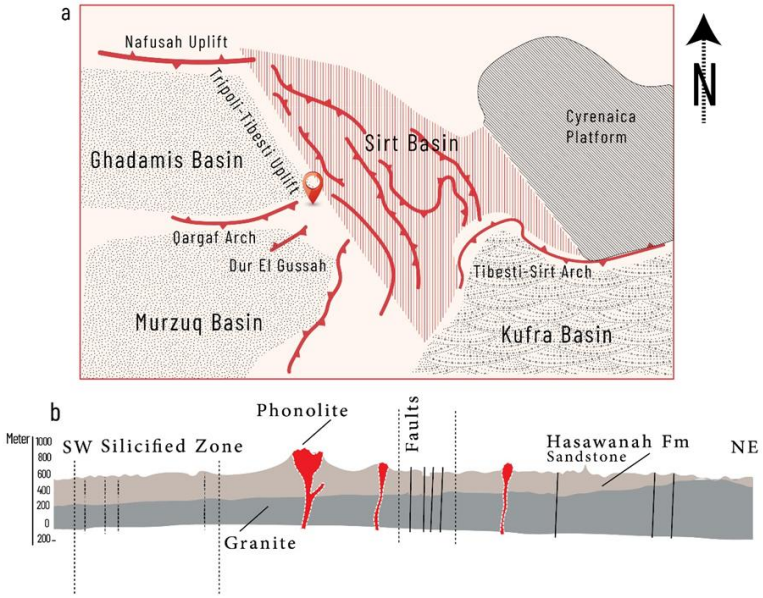

Figure (2): (a). Tectonic map of the study region (b). Cross section of the study area. Modified after Klitzsch, and Ziegert (2000).

The area is generally flat at altitudes ranging from 550 to 600 m, whereas the oldest rock outcrops in the area of Jabal Fezzan are those of the Precambrian complex encountered in the core of a gentle dome arising (Figure 3) and are unconformably overlain by the thick Hasawanah Formation with conglomerates at its base. It consists of basal conglomerate and a thick sequence of sandstone with sporadic thin interbeds of sandy siltstones and quartzites. The observable thickness of the Hasawanah Formation in Wadi Badran is 150 m. In Wadi Badran (Figure 4a-c), metamorphic rocks display schistosity and are predominantly semi- to metapelitic, intruded by granitic rocks during the Late Precambrian Pan-African orogeny, accompanied by metamorphism (Peregi et al., 2003). Moreover, silicified veins and tourmaline are of significant often of meter order of magnitude along the strike and are commonly associated with pegmatic-hydrothermal activities and altered mineral zones (Figure 4d-f). The biotite schist is characterized by a medium to coarse-grained texture, a lustrous silvery appearance, and a foliated structure.

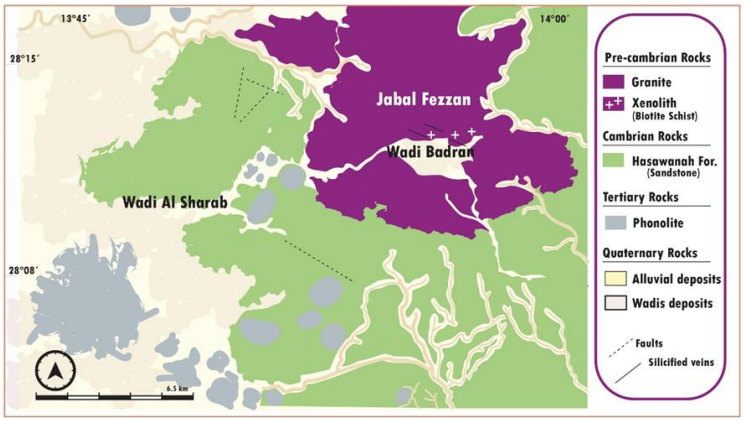

Figure (3): Geological map of the study area. Modified after Jurk, 1978.

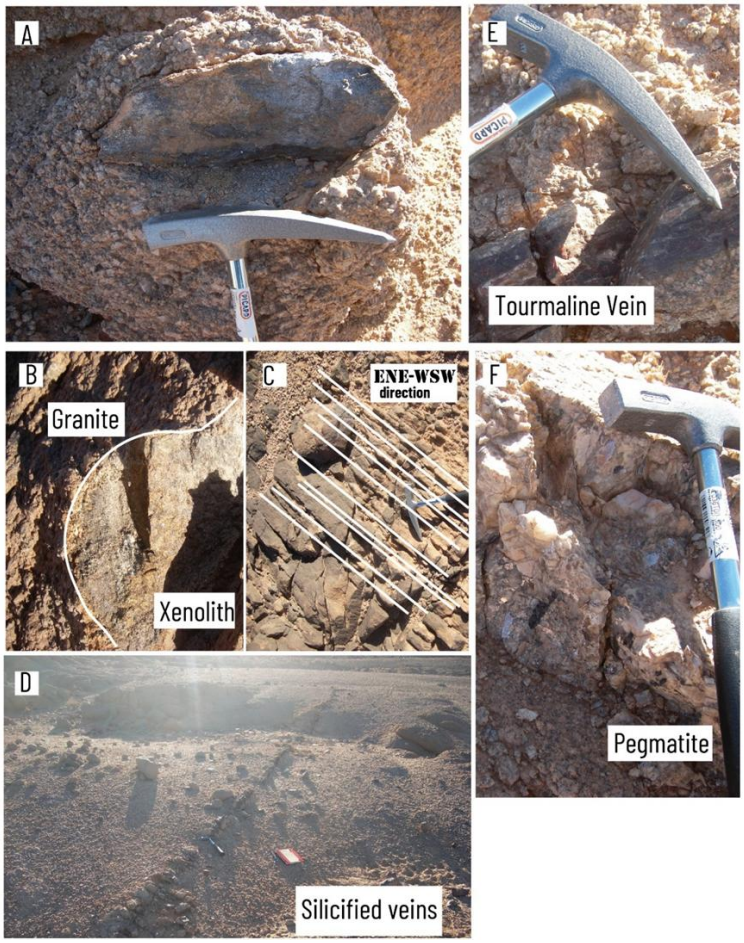

Figure (4): Field photographs: (a). Xenolith outcrop consists of biotite schist different sizes in diameter (b). Biotite schist intruded by Precambrian granite (c). Major-joint sets trending ENE–WSW (d & e). Silicified veins; (f). Pegmatite dike.

Petrography

Wadi Badran pelitic schist is composed predominantly of biotite, forms small hypidioblastic flakes and aggregates of oriented hypidioblastic and xenoblastic crystals (Figure 5a), contain inclusion of quartz, rutil, and opaque minerals, and presents as pseudomorphs. Quartz (Figure 5b) forms typical granoblastic textures and mainly occurs as xenomorphic and interstitial grains.

The grain size is in the range of 0.5x0.3-2.5x1mm (polycrystalline grains are rare). Quartz makes up 20% with middle to fine grain (>5 mm), biotite comprises (35-45%) and muscovite (20–30%) as matrixes. Mineral composition of all the petrologically investigated samples is dominated by K-feldspar (35–50%) microcline perthite. It is euhedral to subhedral and minor plagioclase (20–25%; Figure 5b). Muscovite forms hypidioblastic flakes or small xenoblastic patches in the matrix (Figure 5a). Hornblende

commonly form euhedral idioblastic with elongated prismatic shapes, which can contain inclusion trails that preserve earlier fabrics (Figure 5c). Kyanite forms as bladed crystals and occasionally occurs as masses of crystals and belongs to early events with deformation under burial metamorphism (Figure 5c-d). Feldspar are mainly K-feldspar, with a dominant presence of idioblastic to xenoblastic crystals, which occur in the xenolith matrix and are more and less hydrothermally altered with widespread sericitization.

The accessory minerals (Figure 5e-f) are mainly sphene, zircons were observed in the biotite and plagioclase as inclusion, apatites, sphene and Fe-Ti oxides are most abundant (up to 5% vol., rarely up to 10% vol.,). According to petrological characteristics, the grade of metamorphic changes is generally very low intensity, reflected in orientation and linear distribution of mineral fragments (Figure 6) and very poorly visible, so primary characteristics of the altered rocks are not largely preserved. Foliation, as a real planar fabric element, is marked by parallel orientation of mineral grains and it is poorly developed in low-grade of metamorphism. Biotite displays a well-developed schistosity defined by the preferred orientation of biotite flakes and has a preferred orientation that refers to deformation and crystallization (Figure 6). The samples are characterized by sanidinite-facies metamorphosed pelitic rocks and are typically found as xenoliths inside plutons (Figure 7).

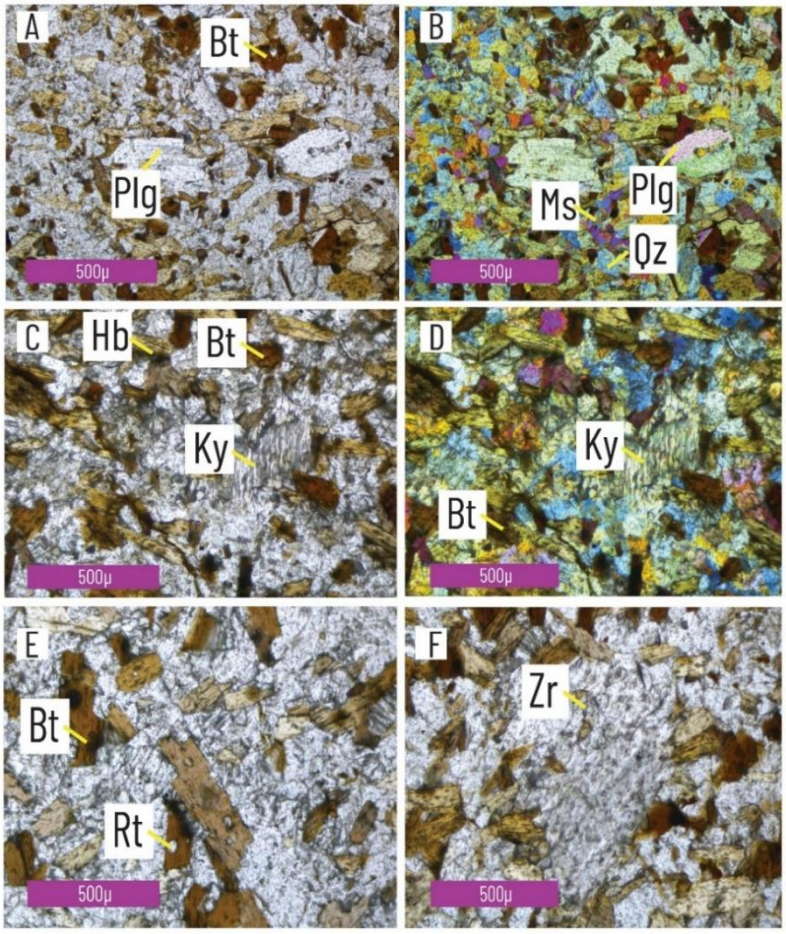

Figure 5: Photomicrographs of biotite schist from Jabal Fezzan. (a). Hypidioblastic xenoblastic crystals of biotite with a black pleochroic halo. (b). Hypidioblastic flakes of muscovite). (c-d). Polarized and photomicrograph of kyanite and poikiloblastic porphyroblasts with elongated prismatic hornblende. (e-f). Secondary minerals (rutile and zircon) occur in variable amounts. abbreviations after Whitney and Bernard Evans (2010).

The biotite schist exhibits a foliation with spherical clusters of biotite (>30%), distinguishes the greenschist facies and indicates a reasonably high degree of metamorphism as it approaches the biotite

zone indicating that it formed as secondary phase of metamorphism during the late hydrothermal activity.

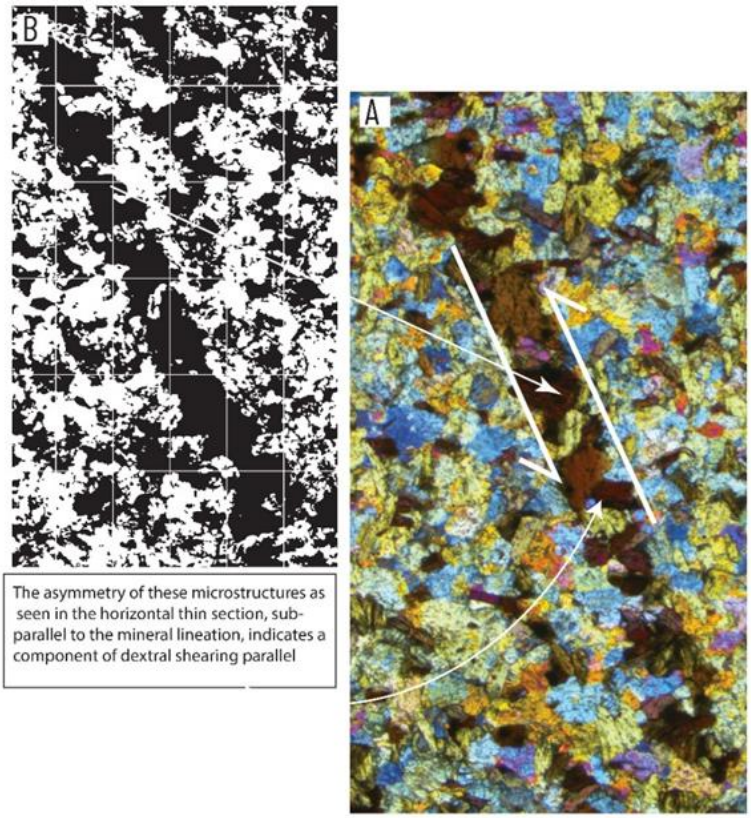

Figure 6: (a). Thin-section studied sample JF-4 showing normal oriented and linear distribution of biotite. (b) higher-resolution image has been placed in the electronic supplement.

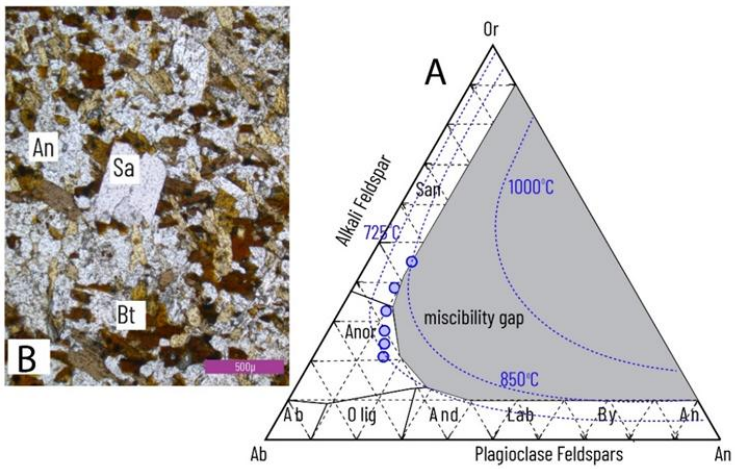

Figure 7: (a). Ternary classification diagram Ab-An-Or for feldspars showing all plagioclases and alkali-feldspar crystals analyzed in the selected samples. The temperature boundary conditions are calculated with thermometers of Fuhrman and Lindsley (1988). (b). Sanidine crystal may appear as either a rim or as an overgrowth of recrystallization with a unique comb-texture composed of plagioclase and alkali-feldspar crystals.

Methods

Fieldwork commenced in Spring 2023 and consisted of transects across Jabal Fezzan. The collection consisted of biotite-schist rocks. All samples were cleaned, sawn, and crushed in preparation for petrographic and geochemical analysis. Thin sections were carried out at the Libyan Petroleum Institute. Rock samples were first crushed using a geological hammer and jaw. After the rock samples

are crushed and sieved. The total volatiles were determined gravimetrically using the method of loss on ignition (LOI); the weight difference after ignition at 105 C˚ and 1000 C˚.

The analyses of major and trace elements were conducted utilizing X-ray fluorescence (XRF) methodology. Fresh portions of samples were subjected to pulverization employing a tungsten carbide or stainless-steel swing mill for a duration of 2 minutes. Two grams of the resultant milled sample were amalgamated with a flux comprising 66% lithium tetraborate and 34% lithium metaborate (5g), with an accuracy of ±0.0002g in weight. The resultant mixture was subjected to fusion in platinum crucibles for 10 minutes at a temperature of 1100°C, utilizing a Phoenix VFD automated fusion apparatus to yield a homogeneous 32 mm glass disk characterized by a lower surface of analytical caliber.

The concentrations of the major elements were ascertained through the comparison of X-ray intensities corresponding to each element against calibration lines constructed from the analysis of established concentrations in 24 internationally recognized standards. The major oxides and trace elements were evaluated utilizing the meta-borate fusion ICP-OES technique, whereas the trace elements, inclusive of rare earth elements (REE), were determined via inductively coupled plasma mass spectrometry (ICP-MS). The analysis was executed on the New Wave NWR-193 excimer laser, which was coupled to a Thermo Xseries 2 quadrupole ICP-MS instrument.

Geochemistry

Major elements

Samples have major element compositions, implying protoliths (table 1). Specifically, they show felsic compositions with consistent SiO_2 contents of 64.25–75.79 wt%, FeOt 2.34–5.78 wt%, CaO 0.85–1.78 wt%, Na_2O 0.89–3.89 wt%, and almost identical MgO, and K_2O contents of 0.73-2.27 and 1.23-3.45 wt%, respectively, whereas the samples exhibit the lowest Mg number of 20.98.

Whole-rock trace element for biotite-schist xenolith

The samples show similar N-MORB-like trace element affinities (Table 1), exhibiting only slight Nb and U enrichments and similar REE concentrations to N-MORB (Table 1). Although the samples have a slightly low Ba/Th ratio (58). All samples are enriched in Pb and Zr relative to N-MORB.

Table 1: Representative chemical analyses of biotite schist from Jabal Fezzan.

Samples	JF1	JF2	JF3	JF4	JF5	JF6
Major elements (wt%)						
SiO2	74.90	72.20	75.79	72.02	64.25	73.47
TiO	0.57	0.45	0.35	0.81	0.23	0.34
Al2O3	16.07	16.89	15.06	18.65	13.38	14.08
FeO	2.56	5.77	2.34	5.78	2.60	3.34
Fe2O3	3.6	6.77	3.68	6.82	4.06	3.22
MgO	0.73	1.09	2.27	0.89	1.34	1.65
CaO	1.32	1.45	1.78	1.68	0.85	1.67
Na2O	2.13	1.65	2.60	0.89	2.85	3.89
K2O	3.45	2.02	3.27	1.23	2.21	3.06
P2O3	0.02	0.67	0.90	0.39	0.01	0.61
CIPW						
Q	9.04	29.48	58.99	33.23	45.9	33.23
Qr	33.68	21.92	4.9	18.2	9.69	18.2
Ab	43.15	20.73	5.92	30.04	27.59	30.04
An	6.55	3.81	2.98	4.33	6.38	4.33
Hy	3.96	10.4	5.22	7.46	4.12	7.46
Mt	5.22	9.82	9.89	5.89	4.67	5.89
Il	1.48	1.75	1.84	1.01	0.87	1.01
Ap	0.51	0.3	0.44	0.49	0.25	0.49
Trace elements (ppm)						
Rb	159	111	149	120	135	113
Nb	34	14	25	18	11	18

Sr	345	212	189	87	305	276
Ba	567	456	314	479	976	865
Zr	167	113	189	327	189	179
Th	5	16	24	4	27	15
Ta	2.89	2.1	1.89	2.12	0.89	0.58
Pb	15	13	27	19	11	10
U	13	17	45	9	14	9
REE (PPM)						
Ce	38.67	64.67	55.31	24.35	15.6	51.6
Y	25	241	22	25	20	15
Cations (wt%)						
Si	6.12	6.12	8.41	1.5	3.88	2.76
Al	9.2	9.52	7.86	10.47	7.5	6.99
Ti	1.3	1.53	0.87	1.62	0.88	0.77
Fe	4.17	4.17	4.17	4.17	4.17	4.17
Mg	1.43	4.13	1.77	0.56	3.23	1.41
Ca	1.15	0.67	0.81	0.6	0.82	1.021
Na	3.8	1.82	2.28	0.52	2.64	2.43
K	4.71	3.76	2.14	0.83	3.08	1.64
Ratios						
Mg#	20.98	29.02	24.43	5.25	34.82	22.67
Ba/Th	49	64.6	12.35	25.69	133	64.22
Th/Ta	31.25	9.09	54.84	48.15	4.5	60

The biotite schist shows variable extents of depletion of Nb, which suggests variable addition of subduction-derived components. A rigorous quantification of the melting processes (i.e., composition of mantle sources) generating the different rock types, is possible as the mantle source compositions (Figure. 8). These conclusions are fully supported by the Th/Ta ratios and Zr composition (Figure. 8). In particular, this figure shows that the influence from subduction components is moderate, comparatively more significant for metasediments.

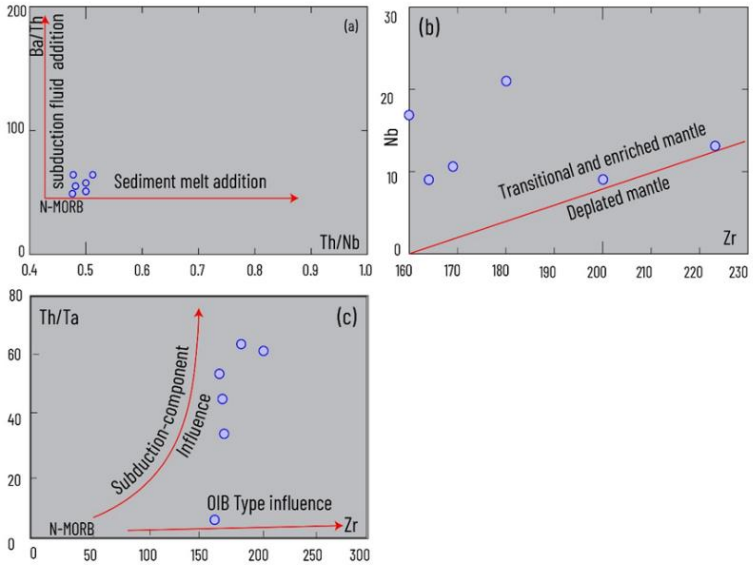

Figure 8:.(a) Ba/Th vs. Th/Nb diagram for biotite schist from Jabal Fezzan after Taylor and McLennan (1985). (b) Nb vs. Zr after Le Maitre (2002). (c). N-MORB and OIB are from Sun and McDonough (1989).

Discussion

Protoliths of the biotite schist xenolith from Jabal Fezzan

A metamorphic process is considered essentially to be an isochemical process, reflecting the mineralogical composition of protoliths, the sediment maturity, and the possible source areas of the metamorphic rock. The Paleozoic rocks in the JF area have been regionally metamorphosed (low-grade, mostly belonging to biotite zones of greenschist facies) during Pan-African orogeny. The field relationship and tectonic situation supports this theory. Source areas composition and tectonic setting were estimated here using the plots proposed by Herron (1988; Figure 9), Foster 1960; Figure 10 a), Peucat et al., (2007; Figure 10b) and Nachit et al., (1985; Figure 10c). Furthermore, the JF samples suggest predominantly are classified as pelites (shales and Fe-Shale), respectively, the samples correspond to ferribiotite and siderophyllite (Figure 10a). Whereas the chemical classification diagram of Nachit et al., (1985) indicates that the Jabal Fezzan xenolith occupies the 're-equilibrated' magmatic biotite (figure 10b).

Likewise, the Fe-Mg*100-Ti*10 triangular diagram shows the nearly linear trend of the samples out of the magmatic trend (Fig. 10c). In addition, Wadi Badran pelitic schist is typically rich in aluminum and is aluminosilicates, including Al_2SiO_5 polymorphs, and is present in high-pressure (e.g., kyanite). In AFM diagrams, the molecular proportions of FeO and MgO are shown as separate components. To determine the plotting parameters for the AFM diagram, we consider A = [Al2O3-3K2O], F = [FeO], and M = [MgO]. With these parameters in place, we can effectively grid the AFM diagram, where the vertical scale is illustrated by the normalized values for the A parameter calculated as [Al2O3-3 K2O]/[Al2O3-3 K2O + FeO + MgO] and the horizontal position is determined by the ratio of MgO/(FeO + MgO). These values were derived following the conversion of the bulk rock chemistry data into molecular proportions (Figure 11). In the AFM diagram (Figure 10) (Nelson 2011), the samples fall into the Andalusite-Kyanite-Silimanite phase and are close to staurolite. However, they have a high Al_2O_3 content (14.18-19.78). Furthermore, they show a relatively variable Al2O3/(FeO+MgO) ratio 2.09-4.24); it is thus possible that the presence of sufficient aluminous minerals in the Al-enriched zone of metasediments depleted in silica.

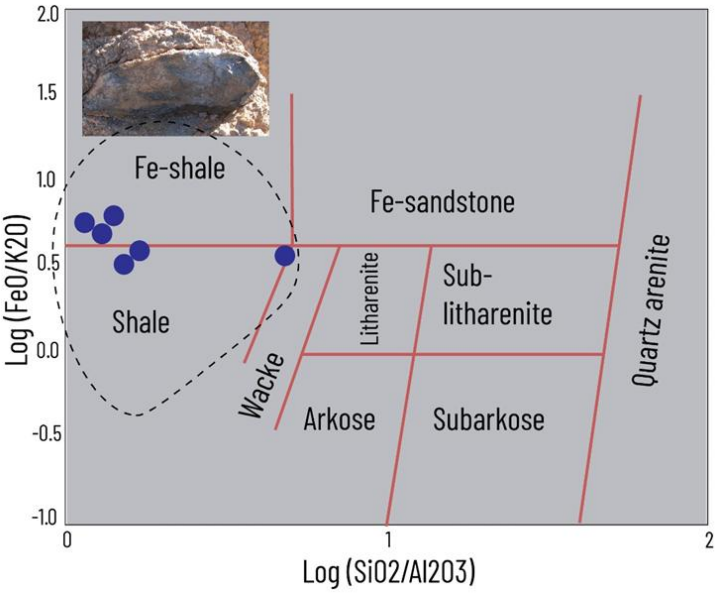

Figure 9: classification diagram of the biotite schist xenolith from Jabal Fezzan [13].

Further, due to the stability of the field of biotite, it is restricted roughly to medium P-T conditions commonly associated with regional metamorphism resulting from crustal thickening during earlier orogenic stages. According to mineral chemistry and textural evidence, the Fe-rich biotite in the metapelitic rocks of the JF is involved in the production and consumption of chemical reactions. As follows, we discuss several reactions: Kyanite is potentially stable at low temperature and pressure. Bucher and Frey (1994) However, under these conditions, the reactions that produce kyanite, such as: Muscovite + staurolite + quartz → biotite + kyanite + H_2O (Spear et al., 1999).

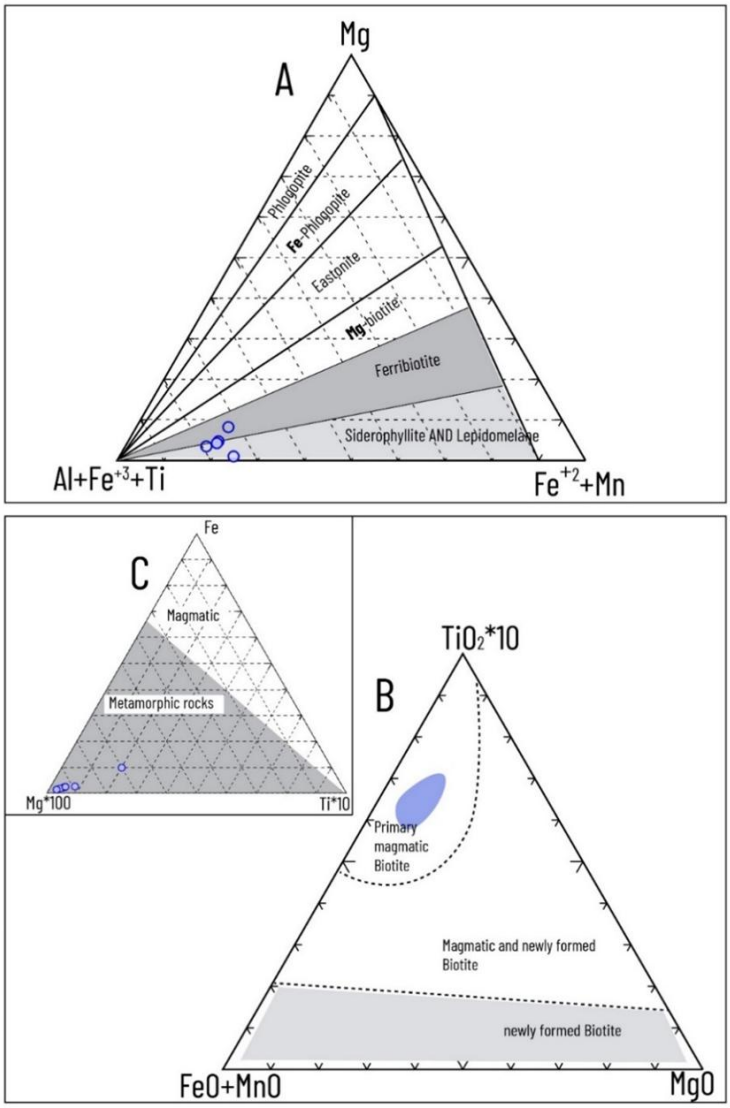

Figure 10: Figure 10. (a) Ternary classification diagram for xenoliths from JB (a) classification diagram for biotite (Foster, 1960). (b) Fe–Mg*100–Ti*10 Peucat et al. (2007) (c) ternary TiO2 -(FeO + MnO)-MgO discrimination diagram (Nachit et al. 1985).

The biotite mineral is formed under greenschist facies conditions by continuous chemical reactions such as chlorite + muscovite = staurolite + biotite + quartz + water. As a result, staurolite growth is either syn-tectonic or post-tectonic to the tectonic activity of the JF metapelitic rocks. As the reaction occurs at pressures greater than about 1.5 kbar, biotite disappears, but kyanite appears (at pressures greater than about 1.5 kbar), and therefore it might be used to define the kyanite isograd if we encountered it in the field. It is possible that the presence of andalusite and sillimanite is related to a superimposed low-P T thermal event in these rocks, although the presence of these polymorphs indicates a pressure below the Al_2SiO_5 triple point, which is placed at 3.8 kbar (Holdaway, 1971). Using Yardley's (1989) equation, staurolite can be converted into sillimanite through reactions such as staurolite + muscovite + quartz; Al2SiO5 (sillimanite) + biotite + water. Due to higher grades of biotite in assemblages free of muscovite, reactions involving muscovite occur at a lower grade than those involving biotite + quartz (Bucher and Frey, 1994).

According to Hofmann et al. (1986), the Nb/U and Ce/Pb ratios of mantle-derived oceanic basalts are consistently low, and deviations may reflect crustal contamination or assimilation (Kieffer et al. 2004). Our samples yield variably low Nb/U (1.5–4.3) and Ce/Pb (0.8–3.59) values, implying possible minor crustal contamination, indicating the strongest crustal influence, the values are variable in our samples, indicating minor crustal contamination. In this study, the pressure-temperature conditions were calculated using standard mineral equilibrium equations.

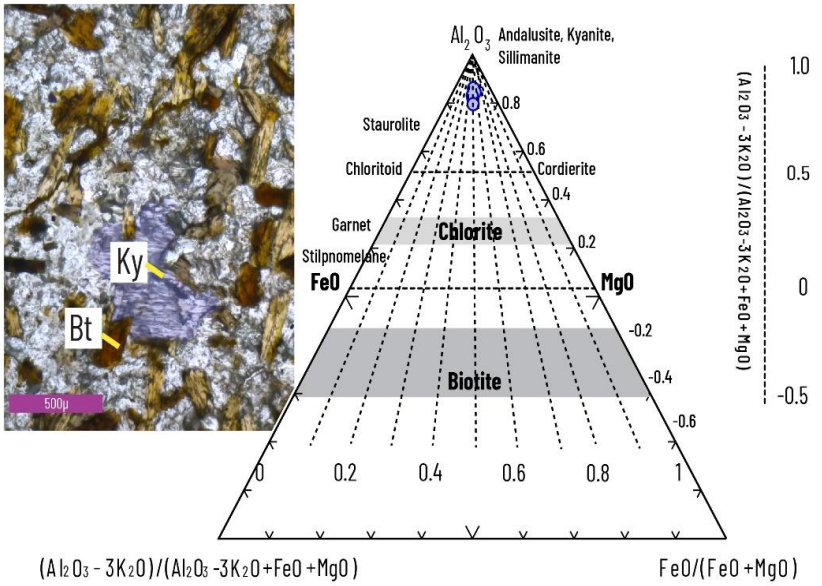

Figure 11: AFM Triangular plots of xenolith from Wadi Badran after Nelson (2018).

The lack of garnet in the assemblages was compensated by using as a close approximation of the garnet composition with the lowest Fe/ (Fe + Mg) and Mn. The pressure-temperature condition of biotite schist from Wadi Badran was considered by using mineral parageneses, reaction textures, mineral assemblages (Biotite (Bt) plagioclase (Plg), Muscovite (Ms) and quartz (qtz). The P-T path of prograde stage passed the reaction of Bt + Qz + H2O +Hlb on 1.5 GPa at 200 ºC to 0.6 GPa at 300 ºC to the peak P-T condition of 300–400 ºC and 1.1–1.22 GPa, which is on the stability field of biotite, muscovite, plagioclase, rutile, and quartz. The estimated peak P-T conditions of biotite-muscovite schist are plotted on the field of green schist-facies (Figure 11). The presence of kyanite in the Jabal Fezzan implies minimum pressures.

Table (2): The result of the thermobarometric data from Wadi Badran.

Sample	P (kbar)	T (℃)	Rock type	Mineral assemblage
JF1	1.23	256	Biotite schist	Bt-Ms-Plg-Qz
JF2	1.1	321	Biotite schist	Bt-Plg-Qz-Hbl
JF3	0.51	350	Biotite schist	Bt-Plg-Qz
JF4	0.43	360	Biotite schist	Bt-Plg-Qz-Hbl
JF5	1.32	289	Biotite schist	Bt-Ms-Plg-Qz
JF6	1.22	376	Biotite schist	Bt-Plg-Qz

The sediments were deposited mainly as (semi-pelites; Oun and Busrewil 2012) during the extension stage of the Sahara Metacraton and were deposited during a long interval of time, probably from the beginning of Mesoproterozoic till the end of Neoproterozoic (ca. 800-600 Ma [1]. Primary rocks were subsequently metamorphosed and tectonically deformed during the final episodes of Pan-African tectono-thermal shaping at the end of the Ediacaran, these rocks were regionally metamorphosed, to varying degrees, in greenschist conditions. Therefore, the rocks were metasomatized (Oun and Busrewil 2012) during the latest Neoproterozoic (ca. 600-530 Ma). Finally, hydrothermal alteration is characterized by a progressive change in phyllosilicate minerals assemblages (Figure 13). This study provides the Sm-Nd isotopic constraints of the Jabal Fezzan xenolith whole-rock Sr, Nd, and Pb isotopic results together with incompatible trace element concentrations, which indicate considerable differences in the extent of trace element among the samples, which lead over time to a wide variety of isotopic signatures in biotite schists. Samples have a radiogenic $^{143}Nd/^{144}Nd$ (~0.5118 Oun et al., 2012; Figure 14), whereas its Pb isotopes are slightly higher than, implying an enriched protolith and the addition of continental crust-like components. Although samples are interpreted as of enriched terrigenous origin, it may have been a low Ba/Th ratio vs. Th/Nb Taylor and McLennan (1985; Figure 8a), which is indicative of dehydration of subducted oceanic crust. Ba/Th ratio is less than 60, which,

together with its radiogenic $^{143}Nd/^{144}Nd$ values (~0.512), shows that the subduction component in the samples is predominantly influenced by sediment melt addition to their mantle sources. These data indicate that the metamorphism in Ediacaran age (Figure 14) and that it was intruded by granitic magmatism. This implies that metamorphism was active during the Precambrian era, much later than subduction initiation in the convergent margin.

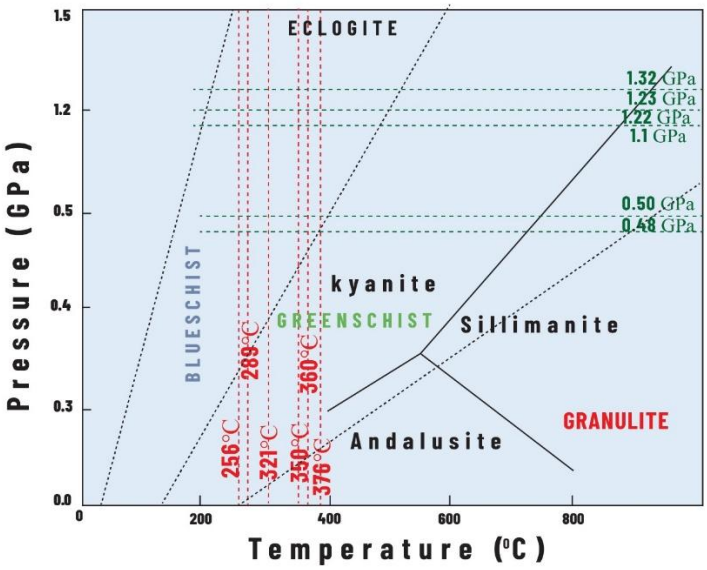

Figure 12: P-T estimation of biotite–schist from Jabal Fezzan. Modified after [38].

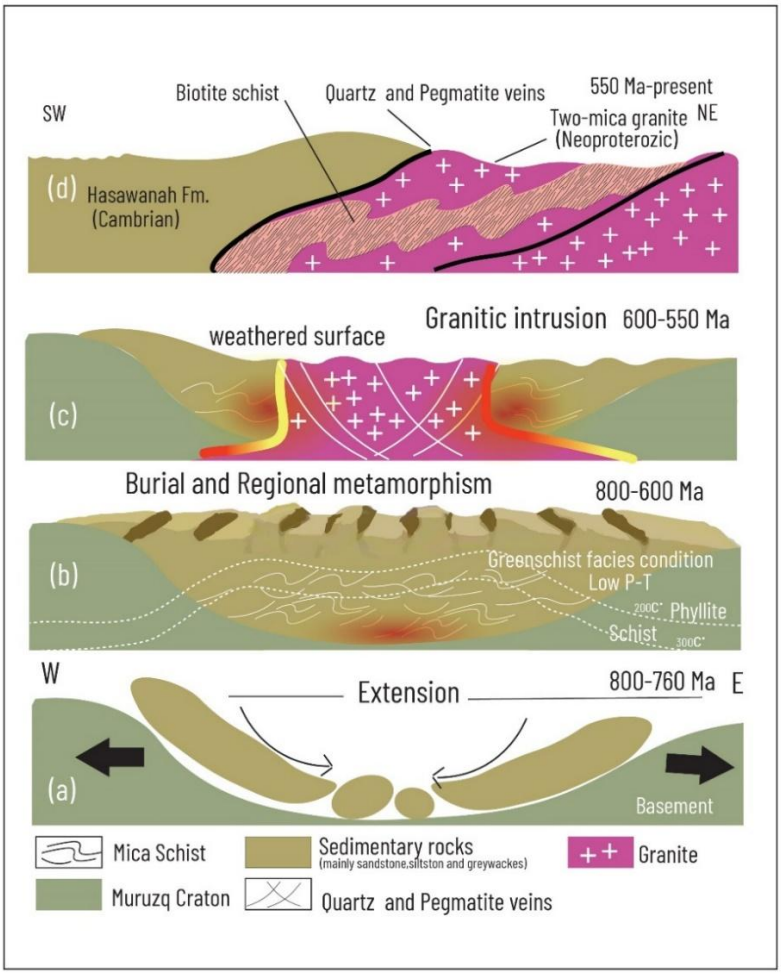

Figure 13: Metamorphic core complex models explain the metamorphism process of biotite schist xenolith.

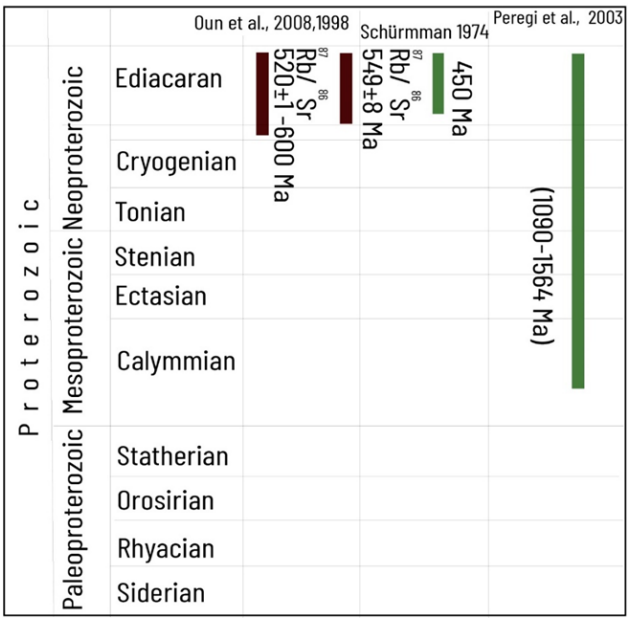

Figure 14: Summary of the geochronological data for biotite-schist, from Jabal Fezzan, southern Libya.

Conclusion

Based on the occurrence and textural relationships of biotite schist with other mineral phases and structural evidence observed in the examined metapelites, the rocks were subjected to complex polymetamorphism and extensive regional metamorphism with increased metamorphic conditions during this period. Metapelites composed of biotite schist were transported and buried at their maximum depth via tectonics, which resulted in crustal shortening and thickening, as well as deformation. It can be attributed to a thermal event superimposed on regional metamorphism that kyanite was formed as a late mineral phase. In addition, metapelites were affected by cooling and retrograde metamorphism as evidenced by several rehydration events. Based on the Nd model ages, it is quite evident that the immature sediments were fed from an old continental source of at least Mesoproterozoic age. More details are needed regarding the study area, particularly in terms of accurately determining the age of the rocks, in order to gain a better understanding of metamorphic rocks and their nature.

Acknowledgments

I extend my sincere thanks to Lisa Fisher for reviewing the paper. The author also extends his thanks to the field guide, Abdel Salam Saad, and the driver, Abu Bakr Al-Hasnawi.

References

1. Abdelsalam G, Liégeois P, Stern J., (2002) The Saharan Metacraton. Journal of African Earth Sciences, 34, 119-136 https://doi.org/10.1016/S0899-5362(02)00013-1
2. Ben sera A., (2024) Petrogenesis of the Neoproterozoic Peraluminous Orogenic Granite and Tertiary Phonolites from Jabal Fezzan in Southern Libya. Petrology 32: 449–466. https://doi.org/10.1134/S0869591124700012
3. Bucher K., and Frey M, (1994) Petrogenesis of Metamorphic Rocks: Complete Revision of Winkler's Textbook, Springer-Verlag, Berlin, pp 319
4. Busreweil M., Oun K, Haman M, (2006) Petrology of the Pan-African basement and Phanerozoic with plate igneous rocks, Sirt Basin. Petroleum Research Journal 19: 27-48
5. Desio, A. (1942). Il Sahara Italiano. II Tibesti nord orientale. Publ. R. Soc. Geogr. Ital., Roma, 232 pp.
6. Desio, A. (1943). L'esplorazione mineraria della Libia. Collezione scientica et documentaria a Cura del Ministro dell'Africa Italiano. Ist. Studi. Int., Milano, 10, 333 pp.
7. El Makhrouf A., Feiss P, (2012) Hornblende Geochemistry and Geobarometry of the post-orogenic granitic plutons Jabal Eghi area, NE Tibisti massif, in: Geology of Southern Libya, 1st edn, Gutenberg press Ltd, Malta, pp 243–266
8. El Makkrouf A, (1988) Tectonic interpretation of Jabal Eghei area and its regional application to Tibesti orogenic belt, south central Libya (S.P.L.A.J.). Journal of African Earth Sciences 7: 945-967

9. Foster M., (1960) Interpretation of the Composition of Trioctahedral Micas: Geological Survey professional paper 354 (B): 1-146.
10. Freulon J, (1964) Etude geologique des series primaires du Sahara central (Tassili n'Ajjer et Fezzan). Centre National de la Recherche Scietifique ser.Geologie 3:186
11. Fuhrman L, Lindsley H., (1988) Ternary-feldspar modelling and thermometry, American Mineralogist 73: 201–215
12. Greigert J, Pougnet F., (1967) Notice explicative sur la carte géologique de la République du Niger à l'échelle du 1.2, 000 000.Editions du Bureau de Recherches Geologues et Minieres. Paris
13. Hoen E., (1968) Geology of the Murzuq basin. Manuscript, American overseas Petroloeum Limited, Tripoli. Libya, pp 85
14. Hofmann W., Jochum P, Seufert M, White M, (1986) Nb and Pb in oceanic basalts: new constraints on mantle evolution. Earth and Planetary Science Letters 79(1): 33–45.
15. Herron, M.M., (1988) Geochemical Classification of Terrigenous Sands and Shales from Core or Log Data. Journal of Sedimentary Petrology, 58: 820-829.
16. Holdaway, M.J., (1971) Stability of Andalusite and the Aluminosilicate Phase Diagram. American Journal of Science, 271: 97-l3l. http://dx.doi.org/10.2475/ajs.271.2.97
17. Jurak L., (1978) Geological map of Libya, 250 000, sheet NH33-14, Jabal Al Hasawnah, Explanatory Booklet, Tripoli Industrial Research Centre, pp180
18. Karpoff R., (1946) Stratigraphie de l'Antacambrian au Sahara.Le Nigritien C.R.Acad.Sci.Paris 233,128p.
19. Kieffer B, Arndt N, Lapierre H, Bastien F, Bosch D, Pecher A, Yirgu G, Ayalew D, Weis D, Jerram A., (2004) Flood and Shield Basalts from Ethiopia: Magmas from the African Superswell. Journal of Petrology 45(4): 793–834
20. Kilian C., (1925) Sure la presence du Silurian a l'est rt au Sud de Ahaggar C.R.Aca.Sci.Paris, pp88
21. Klerkx J., (1980) Age and metamorphic evolution of the Basement complex around Jabal al Awaynat. In: Salem M, Busrewil T (eds) The geology of Libya. 3rd edn. Academic Press, London, III, pp 901-906
22. Klitzsch E., (1970) Die Strukturgeschichte der Zentralsahara Neue Erkenntnisse zum Bau und zur Paläogeographie eines Tafellandes.Geologische Rundschau.59: 459-527
23. Klitzsch E, Ziegert H., (2000) Short Notes and Guidebook on the Geology of the Dor el Gussa-Jabal Bin Ghanimah Area. Sedimentary Basins of Libya, 2nd Symp., Geology of Northwest Libya. ESSL, Tripoli, pp 52
24. Leubre M., (1952) Aprecu sur la geologie du Fezzan.Bull.Sev.Carte Geol.Algerie Trav.Recents. Collab.3: 109-148
25. Le Maitre W., Streckeisen A, Zanettin B, Le Bas J, Bonin B, Bateman P (2002) Igneous Rocks: A Classification and Glossary of Terms: Recommendations of the International Union of Geological Sciences Subcommission on the Systematics of Igneous Rocks (2 ed.). Cambridge University Press, pp 20
26. Mamgain V., (1980) The Pre-Mesozoic (Precambrian to Palaeozoic) Stratigraphy of Libya-A Reappraisal. Department of Geology Research and Mining bulletin No.14. Industrial Research Centre.Tripoli, pp104
27. Menchikoff N., (1962) Carte geologique du Nord-Quest de l' Afrique Sahara central.1:2,000,000, Feuille 4,2nd Ed.Centre de Rech.Sahariannes du CNRS,Paris.
28. Nachit, H., Razafimahefa, N., Stussi, J.M., Carron, J.P., 1985. Composition chimique des biotites et typologie magmatique des granitoiides. Comptes Rendus Acade´mie des Sciences (Paris) 301, 813–818
29. Nelson S., (2018) Earth and Environmental Sciences 2120.Petrology. Lecture materials.
30. Oun K, Busreweil M., (2012) Provenance and metamorphism of Infracambrian (Neoprotereozoic) basement; surface and subsurface oceanic metasediments from Libya.In: Oun K, Busreweil M (ed) Geology of southern Libya 1st edn, Gutenberg press Ltd, Malta, pp153-168
31. Oun K, Mengue J, Himmali A., (1998) Geology, Geochemistry and Tectonic Evolution of the Dur al Gussa Basement interior. Unpublished report, industrial research centre, Tripoli.pp106
32. Peregi Z, Less G, Konrad G, Fodor L, Gulacsi Z, Gyalog, L, Turki S, Suwesi S, Sherif K, Dalub H, (2003) Geological map of Libya.1:250 000.Sheet Al Haruji al Abyad (NG 33-8). Explanatory Booklet.Industrial Research Centre.Tripoli, pp 250

33. Peucat J, Ruffault P, Fritsch E, Bouhnik-Le Coz M, Simonet C, Lasnier B., (2007) Ga/Mg ratio as a new geochemical tool to differentiate magmatic from metamorphic blue sapphires. Lithos 98: 261–274.
34. Spear S, Kohn J., Cheney T (1999) P-T paths from anatectic pelites. Contributions to Mineralogy and Petrology 134: 17-32
35. Schürmann H, (1974) The Pre-Cambrian in North Africa, Brill Archive, pp 351
36. Sun S, McDonough W., (1989) Chemical and isotopic systematics of oceanic basalts: implications for mantle composition and processes. In: Saunders D, Norry J (eds) Magmatism in the Ocean Basin, Geological Society, London, Special Publications 42: 313–345 https://doi.org/10.1144/GSL.SP.1989.042.01.19ز
37. Taylor, S.R. and McLennan, S.M., (1985) The Continental Crust: Its Composition and Evolution. Blackwell, Oxford.
38. Wackrenier P., (1958) Notice explicative de la carte geologique proviso ire du Borkou-Ennedi Tibesti au 1:1,000, 000.Dir. Min.Geol. Brazzavile, pp 24.
39. Whitney L., Evans W (2010) Abbreviations for names of rock-forming minerals. American Mineralogist 95 (1): 185-187
40. Winter D (2001) An Introduction to Igneous and Metamorphic Petrology Prentice-Hall Inc., New Jersey.
41. B. W. Yardley D., (1989). An Introduction to Metamorphic Petrology. xiii + 248 pp. Harlow: Longman; New York: John Wiley